Arming tumor-associated macrophages to reverse epithelial cancer progression

Hiromi I. Wettersten[1,2,3], **Sara M. Weis**[1,2,3], **Paulina Pathria**[1,2], **Tami Von Schalscha**[1,2,3], **Toshiyuki Minami**[1,2,3], **Judith A. Varner**[1,2], **David A. Cheresh**[1,2,3,*]

[1]Department of Pathology, San Diego, La Jolla, USA

[2]Moores Cancer Center, San Diego, La Jolla, USA

[3]Sanford Consortium for Regenerative Medicine at the University of California, San Diego, La Jolla, USA

Abstract

Tumor-associated macrophages (TAMs) are highly expressed within the tumor microenvironment of a wide range of cancers where they exert a pro-tumor phenotype by promoting tumor cell growth and suppressing anti-tumor immune function. Here, we showed that TAM accumulation in human and mouse tumors correlates with tumor cell expression of integrin αvβ3, a known driver of epithelial cancer progression and drug resistance. A monoclonal antibody targeting αvβ3 (LM609) exploited the co-enrichment of αvβ3 and TAMs to not only eradicate highly aggressive drug-resistant human lung and pancreas cancers in mice, but prevent the emergence of circulating tumor cells. Importantly, this anti-tumor activity in mice was eliminated following macrophage depletion. While LM609 had no direct effect on tumor cell viability, it engaged macrophages but not natural killer (NK) cells to induce antibody-dependent cellular cytotoxicity (ADCC) of αvβ3-expressing tumor cells despite their expression of the CD47 "don't eat me signal". In contrast to strategies designed to eliminate TAMs, these findings suggest that anti-αvβ3 represents a promising immunotherapeutic approach to redirect TAMs to serve as tumor killers for late-stage or drug-resistant cancers.

Keywords

Integrin; macrophage; cancer; immunotherapy; monoclonal antibody

Introduction

Integrin αvβ3 is a marker of angiogenic blood vessels in cancer [1, 2], and its expression on tumor cells has been linked to cancer progression, drug resistance, and epithelial-to-mesenchymal transition (EMT) [3, 4]. As such, two primary drugs targeting αvβ3 have advanced to clinical testing, including a monoclonal antibody (etaracizumab) and a cyclic

*Correspondence & Lead Contact: David Cheresh, PhD; University of California, San Diego Department of Pathology and Sanford Consortium for Regenerative Medicine; 2880 Torrey Pines Scenic Drive, Room 4003, La Jolla, CA 92037-0695; Phone: 858-822-2232, Fax: 858-534-8329, Email: dcheresh@ucsd.edu.

peptide antagonist (cilengitide). These agents, while safe, produced only modest clinical activity in the patient populations tested.

Cilengitide, a selective cyclic peptide inhibitor of integrins $\alpha v\beta 3$ and $\alpha v\beta 5$, produced encouraging results in phase 1/2 trials for patients with advanced glioblastoma multiforme [5, 6], yet ultimately failed to meet overall survival endpoints in phase 3 [7]. A subsequent correlative immunohistochemical study revealed that higher $\alpha v\beta 3$ protein levels were associated with improved survival for patients treated with cilengitide [8], suggesting that certain subsets of patients may be particularly sensitive to this drug. In fact, we recently identified a subset of tumors within the "proneural" and "classical" subtypes of glioblastoma that are addicted to aberrant signaling from integrin $\alpha v\beta 3$, making them highly sensitive to agents, including cilengitide, that disrupt the pathway [9]. Thus, it is tempting to speculate that cilengitide would have been able to meet the survival endpoints for a more defined subset of glioblastoma patients.

The monoclonal anti-$\alpha v\beta 3$ antibody etaracizumab has been tested in patients with several types of solid tumors, including a small cohort of patients with metastatic renal cancer where it was able to prolong stable disease for 3 patients [10]. Despite a good safety profile, etaracizumab did not slow disease progression in patients with sarcoma, prostate, or colorectal cancers [10]. Interestingly, this antibody was tested in a phase 2 trial () for patients with metastatic prostate cancer in combination with standard of care docetaxel, prednisone, and zoledronic acid. Notably, steroids such as prednisone have been associated with inferior immunotherapy responses [11], while zoledronic acid can block the activity of M2 macrophages [12]. Similarly, etaracizumab was tested in a phase 2 trial for melanoma in combination with the standard of care, dacarbazine [13]. In this trial, the overall survival for patients treated with etaracizumab was 12.6 months, while patients treated with etaracizumab plus dacarbazine had a worse overall survival (9.4 months), compared with historical data for dacarbazine alone (6–10 months) [13]. In addition to acting as a cytotoxic agent for tumor cells, dacarbazine also produces immunosuppressive effects within the tumor microenvironment, including inhibition of M2 macrophage activity [14]. Together, these clinical trial results suggest that the monoclonal antibody etaracizumab may improve survival in the context of immune effector cells.

Monoclonal antibodies have emerged as a class of anti-cancer therapeutics to not only directly kill tumor cells, but to manipulate anticancer immune responses [15]. The activity of several FDA approved anti-cancer antibodies such as anti-CD20 (Rituximab) and anti-EGFR (Cetuximab) have been attributed to their ability to induce antibody-dependent cellular cytotoxicity (ADCC) [16, 17]. This process is triggered when antibodies bind to tumor cell antigens and are simultaneously recognized by Fcγ receptors on immune effector cells, including natural killer (NK) cells, monocytes, macrophages, neutrophils, and dendritic cells [18].

While not present in early stage disease, integrin $\alpha v\beta 3$ becomes enriched during epithelial cancer progression, in particular as tumors lose sensitivity to standard of care [19]. As such, integrin $\alpha v\beta 3$ represents an ideal tumor antigen to mount an attack against. Here, we show that $\alpha v\beta 3$ on epithelial cancers positively correlates with the accumulation of tumor-

associated macrophages (TAMs) within the tumor microenvironment, immune cells that typically lead to tumor progression and immune suppression. Interestingly, TAMs armed with an anti-αvβ3 antibody can be activated to kill the highly aggressive αvβ3+ CD47+ epithelial cancer cells via ADCC and thereby suppress cancer progression and drug resistance. Our work reveals a potentially valuable subpopulation of patients who might be particularly sensitive to the effects of an αvβ3-targeted antibody, namely those with advanced epithelial cancers whose tumors have become co-enriched for integrin αvβ3 and TAMs.

Materials and Methods

Statistics

Testing for normality was performed using Shapiro-Wilk Test. Student's *t*-test, Mann-Whitney U test, One-sample *t*-test, or ANOVA was performed to compare independent sample groups. Pearson's or Spearman's correlation was used to measure correlation of multiple groups. Excel (Microsoft) and SPSS (IBM Analytics) were utilized for analysis.

Cell lines

Cells were grown in DMEM unless stated. Mouse lung cancer (LLC), human lung adenocarcinoma (HCC827 and H1975, grown in RPMI), human renal cell carcinoma (A498), and human pancreatic carcinoma cells (PANC-1) were obtained from the American Type Culture Collection (ATCC). PC9 lung adenocarcinoma cells were a gift from Dr. Joan Massague (Sloan-Kettering Institute, USA). Cell line authentication was performed by the ATCC using short tandem repeat DNA profiles. FG (COLO-357) pancreatic carcinoma cells, were a gift from Dr. Shama Kajiji and Vito Quaranta (The Scripps Research Institute). CW389 glioblastoma cells (grown in neurobasal media) were provided by Dr. Jeremy Rich (UC San Diego). Upon receipt, each cell line was expanded, cryopreserved as low-passage stocks, and tested for *Mycoplasma* using MycoScope PCR Mycoplasma Detection Kit (Genlantis, MY01050). All the cell lines were used within 30 passages. For ectopic expression and genetic knockdown, cells were transfected with a vector control, integrin β3, or luciferase using a lentiviral system as previously described [19, 20]. For genetic knockout, β3 gRNA and Cas9 were transfected using Lipofectamine 3000 (Thermo, L3000001). gRNA sequences are listed in Supplemental Table 1.

Reagents, chemicals, and antibodies

Fab LM609 was a gift from Dr. Marija Backovic (Pasteur Institute). Control and clodronate liposomes were obtained from ClodronateLiposome.com. Captisol (Cydex) was diluted in water at 6%. Erlotinib (Selleckchem, OSI-744) was diluted in DMSO for *in vitro* or Captisol for *in vivo* experiments. Anti-αvβ3 antibody, LM609, was produced as previously described [21]. Batch to batch activity is confirmed by adhesion assays. Antibodies are listed in Supplemental Table 1.

Gene expression analysis using public databases

mRNA expression in TCGA datasets was used to analyze the correlation between *ITGB3* and immune cell type scores, calculated as previously described [22] using cBioPortal. Gene sets for immune cell markers are listed in Supplemental Table 2.

Correlation analysis of ITGB3 and immune cell types using NanoString nCounter

10 pre-existing, de-identified lung adenocarcinoma frozen tissue biopsies were obtained from the Moores UCSD Cancer Center Biorepository. mRNA was extracted using the RNeasy Mini Kit (Qiagen, 74104). The quality of extracted mRNA was tested using Agilent Bioanalyzer (Agilent). Expression of mRNAs involved in immune cell activities was analyzed using nCounter® PanCancer Immune Profiling Panel (NanoString).

Protein analysis

Immunohistochemical staining—Immunohistochemical staining was performed on FFPE slides using the VECTASTAIN Elite ABC HRP Kit (Vector, PK-6100), ImmPRESS Excel Staining Kit (Vector, MP-7602), and ImmPRESS HRP anti-rat IgG, mouse adsorbed (peroxidase) polymer detection kit (Vector, MP-7444). Slides were imaged on a NanoZoomer Slide Scanning System (Hamamatsu), and the area fraction for each protein with respect to tumor tissue was calculated utilizing ImageJ (NIH) [23]. Integrin β3 levels on tumor cells for cancer microarray slides were analyzed blindly, and the tissues were categorized into β3- and β3+ groups. Microarray slides were purchased from Biomax.us: Lung cancer (LC10011a, 50 cases/100 cores, grades 2–3; LC121c, 120 cases/120 cores, grades 1–3; HLugC120PT01, 60 cases/60 cores, grades 1–3), Prostate cancer (PR483c, 48 cases/48 cores, grades 1–3), Colon carcinoma (CO1006, 50 cases/100 cores, grades 1–3), Kidney clear cell cancer (Hkid-CRC060CS-01, 30 cases/60 cores, grades 1–4; BC07001, 40 cases/80 cores, grades 1–3), Multiple organs (MC1801, 180 cases/180 cores, containing 26 cases of colon, pancreas, lung, breast and prostate cancer, grades 1–3) and Brain glioblastoma (GL805, 40 cases/80 cores, grades 3–4).

Immunofluorescence staining—Immunofluorescence staining was performed on frozen sections permeabilized with 0.1% TritonX-100 (Bio-Rad, 1610407) in PBS for one minute, blocked with 10% NGS (Jackson ImmunoResearch, 005–000-121) in PBS for two hours, and incubated with DAPI (Life Technologies, 62248, 1 μg/mL in 1% BSA in PBS) and an anti-mouse F4/80 antibody (eBioscience 14–4801-82, conjugated with Texas Red fluorophore by OneWorldLab) for two hours at room temperature. Images were acquired utilizing a Nikon Eclipse C2 confocal microscope (Nikon). F4/80-positive area fraction with respect to tumor tissue was calculated utilizing ImageJ (NIH) [23].

Flow cytometry—Cell pellets were washed with PBS, blocked with 1% BSA in PBS for 30 minutes at room temperature and stained with indicated primary antibodies or IgG isotype controls with or without fluorescently labeled secondary antibodies. Cells were incubated with propidium iodide (Sigma, P4864), then flow cytometry was performed on a BD LSRFortessa™ and analyzed using FlowJo (Treestar) software.

In vitro functional assays

MTT (cell viability) assay—Cells in 96-well plates were incubated in thiazolyl blue tetrazolium bromide solution (Sigma, M2128) for two hours at 37°C. After the solution was removed, the blue crystalline precipitate in each well was dissolved in DMSO. Visible absorbance at 560 nm was quantified using a microplate reader.

Antibody-dependent cellular-cytotoxicity (ADCC) assay—Target cells stained with CFSE Cell Division Tracker Kit (BioLegend, 423801) were co-cultured with effector cells with or without isotype IgG or LM609 for 5–16 hr at 37°C, stained with PI, and flow cytometry was performed on BD LSRFortessa™. The ratio of dead target cells (PI-positive) to the total target cell population (CFSE-positive) was calculated as described [24].

Antibody-dependent cellular phagocytosis (ADCP) assay—Target cells stained with CFSE Cell Division Tracker Kit (BioLegend, 423801) were co-cultured with effector cells stained with CellTrace™ Far Red Cell Proliferation Kit (Thermo, C35464), with or without isotype IgG or LM609 for 5 hr at 37°C. The ratio of CFSE-Far Red double positive cells was calculated using flow cytometry as described [24].

Mouse tumor experiments

Study approval—All experiments involving mice were conducted under protocol S05018 approved by the UC San Diego Institutional Animal Care and Use Committee. All studies are in accordance with the NIH Guide for the Care and Use of Laboratory Animals.

Isolation of tumor-associated macrophages (TAMs) from mice—TAMs were isolated from tumor tissues as described [25]. Tumors were dissociated in HBSS containing collagenase IV (Sigma, C5138), hyaluronidase (Sigma, H2654), dispase ll (Roche, 04942078001), and DNase IV (Millipore, D5025) at 37°C for 15 minutes. Cell suspensions were filtered through 70 μm cell strainers and washed with PBS. Single cell suspensions (10^6 cells/100 μL in 5% BSA in PBS) were incubated with Mouse BD Fc Block™ (BD Biosciences, 553142, 1:50) for 10 minutes at 4°C and fluorescently labeled antibodies, CD11b (eBioscience, 17–0112-81, 1:100), and Ly-6G (eBioscience, 25–5931-81, 1:100), for one hour at 4°C. TAMs (CD11b-positive, Ly-6G-negative) were sorted.

Isolation of bone marrow derived macrophages (BMDMs) from mice—BMDMs were aseptically harvested from euthanized 8–10 week-old female C57BL/6 mice by flushing leg bones with RPMI, filtering through 70 μm cell strainers, and incubating in Red Blood Cell Lysing Buffer Hybri-Max™ (Sigma, R7757). Cells were incubated with mouse M-CSF (Peprotech, 315–02) for 7 days before ADCC assays.

Isolation of NK cells from mice—Splenocytes were aseptically harvested from euthanized 8–10 week-old female C57BL/6 mice by mincing spleens with PBS containing 2 % FBS and 1 mM EDTA, filtering through 40 μm strainers, and incubating in Red Blood Cell Lysing Buffer Hybri-Max™ (Sigma, R7757). NK cells were isolated from splenocytes using NK Cell Isolation Kit II (Miltenyi, 130–096-892).

Isolation of human peripheral blood mononuclear cells (PBMCs) and macrophages—Leukoreduction system chambers (LRSC) were purchased from the San Diego Blood Bank. PBMCs were isolated from LRSC using Histopaque-1083 (Sigma, 10831) following the manufacturer's protocol. To obtain macrophages, PBMCs were incubated in tissue culture plates with human M-CSF (Peprotech, 300–25) for 5 days.

Genotyping of FcγR polymorphism—Genomic DNA was isolated from donor blood using Genomic DNA Mini Kit (Invitrogen, K1820–00). DNA was analyzed for FcγRIIa (rs1801274) and IIIa (rs396991) polymorphisms using TaqMan SNP Genotyping Assays (Life Technologies, 4351379).

Isolation of erlotinib-resistant tumor cells from mouse tumors—Erlotinib resistant HCC827 (HCC827-R) cells and PC9 (PC9-R) cells were established as previously described [19].

Xenograft model with macrophage depletion—5 million human pancreatic carcinoma (FG+β3) or human lung carcinoma (HCC827+β3) cells in 100 μl PBS were subcutaneously injected to the right flank of female nu/nu mice (Charles River, #088, 8–10 weeks old). Twice weekly, body weight was monitored and tumors measured with calipers (Volume = 1/2 length × width^2). Animals with an average tumor volume of 150 mm^3 were randomly assigned into groups treated i.p. twice per week with combinations of control or clodronate liposome (200 μL) and LM609 (10 mg/kg) or vehicle control (PBS). Harvested tumor tissues were fixed in 10% formalin or frozen in OTC compound (VWR, 25608–930). The percent of monocytes in blood for nu/nu mice is 4.31% compared with 4.37% for C57BL/6 mice (Charles River, Biochemistry and Hematology for Mouse Colonies in North America).

Lung xenograft model with acquired resistance to erlotinib—An erlotinib resistant lung adenocarcinoma xenograft model was utilized as previously described [26]. Briefly, HCC827 ($5 × 10^6$ tumor cells in 100 μl of PBS) cells were subcutaneously injected to the right flank of female nu/nu mice (Charles River, 088, 8–10 weeks old). Tumors were measured with calipers twice per week. Animals with a tumor volume of 250–700 mm^3 were randomly assigned into groups treated with combinations of Captisol (oral, six times/ week), PBS (i.p., twice/week), LM609 (i.p., 10 mg/kg, twice/week), or erlotinib (oral, 6.25 mg/kg, six times/week). Vehicle-treated mice were sacrificed on day 15 due to large tumor size, and erlotinib groups on day 50. Tumors were placed into liquid nitrogen, OCT compound, or 10% formalin. Alternatively, Erlotinib sensitive HCC827 (HCC827-P) and PC9 (PC9-P) and resistant HCC827 (HCC827-R18) and PC9 (PC9-R4L) cells were isolated. Tumor growth and αvβ3 expression are shown in Supplemental Figure 3.

Orthotopic lung adenocarcinoma xenografts and CTC isolation—Luciferase- and GFP-positive HCC827 cells ($5 × 10^6$ cells in 50 μl of PBS) were injected into the lungs of female nu/nu mice (8–10 weeks old) and tumor growth monitored by bioluminescence imaging (IVIS Spectrum). Eight weeks after injection, mice were randomly divided into groups: vehicle (6% Captisol, oral, six times/week), erlotinib (oral, 6.25 mg/kg, six times/ week), or the combination of erlotinib and LM609 (i.p., 10 mg/kg, twice/week). Whole

blood (0.5 mL/mouse) was collected in EDTA tubes, and PBMCs including CTCs were isolated using Lymphoprep™ (STEMCELL Technologies, 07801) and SepMate™ (STEMCELL Technologies, 15415). Cells were washed with PBS, plated on poly-L-Lysine coated 8-well chamber plates, fixed with 4% PFA, and stained with DAPI (1 μg/mL in 1% BSA in PBS), LM609 (5 μg/mL in 1% BSA in PBS), and a fluorescently-labeled secondary antibody. The number of αvβ3+ and αvβ3- CTC (DAPI+/GFP+) were counted using a Nikon Eclipse C2 confocal microscope (Nikon).

Results

Integrin αvβ3 positively correlates with macrophage markers across multiple cancers

During cancer progression, the tumor microenvironment becomes dramatically altered with the appearance of various stromal and immune cells that influence the malignant behavior of the tumor [27, 28]. Accordingly, it is important to consider what immune cells are available when targeting tumors with therapeutic antibodies. Although the enrichment of integrin αvβ3 in tumor cells is a driver of an aggressive, drug resistant tumor phenotype [20, 26], the impact of αvβ3-positive tumor cells on the tumor immune microenvironment has not been well defined. We therefore queried multiple TCGA datasets to identify whether β3-expressing tumors may be enriched for certain immune effector cell types that could contribute to antibody-mediated killing. This analysis reveals that mRNA expression of *ITGB3* positively correlates (rho 0.3) with marker sets for macrophages (MΦ), dendritic cells (DC), and neutrophils (NΦ), but not with NK cells (NK) for certain types of solid tumors (Figure 1A). For example, *ITGB3* mRNA expression positively correlates with macrophage markers for kidney, breast, GBM, lung, stomach, prostate, pancreas, esophageal, and colorectal cancers, while no correlation is observed for renal papillary, sarcoma, thyroid, melanoma, and ovarian cancers (Figure 1A). Also, ITGB3 positively correlates with other immune cell types such as mast cells, T cells and B cells, but this relationship is observed for a limited number of tumor types (Figure S1A). Interestingly, no correlation between *ITGB3* and immune cell markers is observed for thyroid, melanoma, kidney papillary, and sarcoma despite these cancers having the highest median expression of *ITGB3* across the TCGA pan-cancer dataset (Figure S1B).

The positive correlation of β3 and immune cell type markers was validated for an independent tumor sample set of 10 frozen lung adenocarcinoma biopsies analyzed using the NanoString nCounter platform (Figure 1B). Even for this modest sample size, tumors with above median *ITGB3* expression are enriched for markers characterizing macrophages, dendritic cells, and neutrophils (but not NK cells) compared with tumors having below median *ITGB3* expression. Consistent with the analysis of TCGA datasets, there is a strong positive correlation between *ITGB3* and these marker sets. Together, these data suggest that β3-positive epithelial cancers may be enriched for multiple cell types that could serve as effector cells for antibody-mediated therapy.

To further validate the positive correlation of the enrichment of macrophages with β3 expression on tumor cells at the protein level for a variety of genetically and histologically distinct solid tumor types, we performed immunohistochemical staining for a series of commercially available tumor microarray slides. This analysis reveals that integrin β3

protein expression on tumor cells positively correlates with the presence of macrophage markers CD68 and CD163 for lung, prostate, colorectal, kidney, and glioblastoma tumors (Figure 1C). Higher magnification images show that individual areas with integrin β3 staining on tumor cells are enriched for cells that stain positive for the macrophage markers (Figure S2). Notably, the percent of tumors with positive tumor cell expression of β3 ranges from 29–54% among the array slides examined, indicating there is a significant portion of β3+ tumors across this diverse population of tumor types, grades, and stages. Together, these findings indicate that tumors with high tumor cell expression of integrin β3 are particularly enriched for TAMs, a component of the tumor microenvironment that contributes to tumor progression [29], and that these cells might prove important when targeting tumors with certain therapeutic antibodies.

An anti-αvβ3 monoclonal antibody triggers macrophage-mediated tumor cell killing

Considering the co-enrichment of TAMs and integrin αvβ3-expressing tumor cells, we reasoned that exploiting this relationship could provide a basis for a therapeutic strategy to treat αvβ3+ cancers. To do this, we used a function blocking monoclonal antibody we previously developed, LM609, which recognizes integrin αvβ3 on human but not mouse cells [30] and served as the parent antibody for a fully humanized version, Vitaxin/etaracizumab [31, 32]. Indeed, we find that αvβ3-expressing human lung and pancreatic xenograft tumors growing in nude mice are highly sensitive to LM609, and that this effect can be completely blocked by macrophage depletion using clodronate liposomes (Figure 2A), demonstrating that TAMs play a critical role in the anti-tumor efficacy of this tumor-targeted antibody.

An enrichment of TAMs has been observed following cancer therapy, including the EGFR inhibitor erlotinib [33], and we previously reported that integrin αvβ3 is upregulated during the acquisition of erlotinib resistance in lung cancers in mice and for the BATTLE trial in man [19]. Accordingly, we show that αvβ3-negative HCC827 human EGFR mutant lung tumors not only gain αvβ3 as they become drug resistant, but they also become enriched for TAMs (Figure 2B). As expected, LM609 alone has no effect on the growth of HCC827 xenograft tumors prior to the development of drug resistance due to lack of the αvβ3 antigen (Figure 2C). While mice treated with erlotinib alone show an initial reduction in tumor size, this is followed by an eventual tumor re-growth and gain in αvβ3 expression (Figure 2C). In contrast, the combination of erlotinib plus LM609 prolongs drug sensitivity and prevents the appearance of integrin β3 (Figure 2C). Interestingly, this combined treatment does not reverse the macrophage enrichment that emerges during erlotinib treatment (Figure S3B).

Since the appearance of circulating tumor cells (CTC) represents a hallmark of tumor progression and EMT [34, 35], we considered whether LM609 might suppress this indicator of aggressive disease. Whereas orthotopic HCC827 lung tumors gain αvβ3 expression during erlotinib therapy and show a marked increase of CTCs in the blood after 4 weeks of therapy, combining LM609 with an EGFR inhibitor prevents the appearance of CTCs in this setting (Figure 2D). Together, our results indicate that the monoclonal antibody LM609 requires macrophages for its anti-tumor activity in mouse xenograft models, and we demonstrate its efficacy for both highly aggressive tumors with constitutive αvβ3 expression

as well as those that gain αvβ3 during acquired resistance to therapy. Moreover, by eliminating those tumor cells that become enriched for αvβ3 during EGFR inhibitor treatment, we can suppress cancer progression as measured by a decrease in the appearance of CTC.

LM609 induces macrophage-mediated antibody-dependent cellular cytotoxicity (ADCC) rather than phagocytosis

To confirm that the mechanism of action for LM609 is macrophage dependent, we asked whether LM609 can kill tumor cells in vitro using TAMs, an abundant source of immune effector cells that are co-enriched with β3 (Figure 1) and which typically play a pro-tumor role [36]. Indeed, LM609 shows robust activity using TAMs isolated from mouse Lewis lung carcinoma (LLC) tumors grown in immune-competent C57BL6 mice or immune-compromised athymic nude mice (Figure 3A). The antibody can also kill tumor cells using human monocyte-derived macrophages isolated from healthy donor blood, as well as bone marrow derived macrophages (BMDM) isolated from healthy mice (Figure 3B, S4A). Binding of the antibody to Fc receptors on macrophages is critical for its killing capacity, since there is no macrophage-mediated killing in the presence of an antibody blocking of the Fc receptors CD16, CD32, and CD64, and a form of LM609 lacking the Fc portion (Fab LM609) cannot trigger macrophage-mediated killing (Figure 3C–D). To our surprise, LM609-mediated ADCC is not achieved with mouse NK cells or peripheral blood mononuclear cells (PBMCs) isolated from human blood (Figure 3E), immune effector cell types to which antibodies are commonly engineered for optimal binding [37, 38]. In fact, NK cells are not correlated with β3 expression in tumors (Figure 1). Together, these findings suggest that the anti-tumor activity of LM609 involves the opsonization of αvβ3-expressing tumor cells with the monoclonal antibody, followed by the subsequent engagement of macrophage Fc receptors to induce killing.

Monoclonal antibodies can direct macrophages to induce tumor cell killing through two primary mechanisms, processes known as antibody-dependent cellular phagocytosis (ADCP) and antibody-dependent cellular cytotoxicity (ADCC). Here, we show that LM609 induces macrophage ADCC, but not ADCP or direct killing, and this requires integrin β3 expression (Figure 3F and S4B–C). The lack of an ADCP response is consistent with high tumor cell expression of CD47, the "don't eat me" signal [39] that tumor cells often exploit to evade phagocytosis (Figure 3F and S4B). Although αvβ3 and other integrins are binding partners for CD47 [40], CD47 expression is not impacted by β3 ectopic expression or knockout (Figure 3F and S4B). Macrophage-mediated ADCC but not ADCP or direct killing is also observed for additional αvβ3-expressing tumor cell lines representing tumor types for which *ITGB3* expression is linked to macrophage enrichment (Figure 1), including lung, pancreas, brain, and kidney cancer (Figure 3G). We also show that LM609 can induce macrophage-mediated ADCC for the drug resistant cells, but not drug sensitive cells, suggesting that the prevention of drug resistance seen in Figure 2C is due to macrophage ADCC (Figure 3H). Taken together, our findings demonstrate that the anti-tumor activity of LM609 results from its ability to engage αvβ3 on tumor cells along with Fcγ receptors on macrophages isolated from peripheral blood monocytes, healthy bone marrow, or tumor

tissues to kill αvβ3-positive tumor cells, including those from a subset of cancers for which *ITGB3* expression is co-enriched with macrophage markers.

Discussion

Our findings that the antitumor properties of LM609 depend on macrophages and their ability to initiate ADCC suggests a new therapeutic strategy for a range of epithelial cancers. Humanized versions of LM609 (MEDI-522, Vitaxin, or etaracizumab) have been tested in phase 1 clinical trials and were shown to be relatively non-toxic [10, 13, 32]. However, in phase 2 trials melanoma patients with etaracizumab alone resulted in a 12.6 month overall survival rate which was decreased to 9.4 months when combined with dacarbazine, a highly immune-suppressive drug that inhibits macrophage activation [13], suggesting that immune cells may contribute to the increased survival observed for patients treated with the antibody alone. Indeed, we show that depletion of macrophages using clodronate liposomes dramatically reduces the therapeutic effect of LM609 in lung or pancreas tumors in mice. Furthermore, our observation that αvβ3 and macrophage markers are not co-enriched in the TCGA melanoma dataset also suggests that melanoma patients may not be the ideal population for a drug like LM609 that exploits this relationship. Instead, we show the potential of combining LM609 with a first-line therapy such as EGFR blockade to prolong drug sensitivity by eliminating drug resistant αvβ3+ tumor cells (Figure 2C) and suppress tumor progression as measured by the elimination of CTCs (Figure 2D). Together, these results indicate that the enrichment of TAMs in αvβ3-expressing tumors renders them amenable to a therapeutic approach that redirects the pro-tumor immune effector cells to attack the tumor.

Our findings provide a general rationale for focusing future efforts on the development of monoclonal antibodies capable of recruiting macrophages. In the tumor microenvironment, the anti-tumor function of cytotoxic T cells and NK cells are compromised, while the recruitment and expansion of pro-tumor macrophages is enhanced [41]. TAMs secrete growth factors and cytokines to promote tumor progression through induction of angiogenesis, metastasis, and immunosuppression [25, 28, 36, 42, 43]. As observed for EGFR inhibitor resistant lung adenocarcinoma patient tumors [33, 44], we find that drug-resistant tumors contain more TAMs than tumors from vehicle-treated mice (Figure 2B). Thus, a strategy to arm macrophages to attack tumor cells may be particularly useful for drug-resistant cancers. Although therapeutic antibodies are commonly screened in vitro for their ability to engage Fc receptors on NK cells, we reasoned that an antibody capable of engaging macrophages may provide a more powerful therapeutic strategy for αvβ3-expressing tumors that feature an abundance of TAMs. Furthermore, considering that PD-L1 (CD274) expression is positively correlated with *ITGB3* in many of those cancers that had ITGB3-macrophage marker positive correlation (Figure S1A), this therapeutic strategy may ultimately provide efficacy in combination with a PD-L1 inhibitor.

The mechanism of action we show for LM609 is fundamentally different than a number of recent strategies to "target" macrophages by blocking their tumor-promoting activities or exploiting potential anti-tumor effector functions [45]. Our data suggests that exploiting TAMs as effector cells for antibody killing does not require a certain macrophage

phenotype, since ADCC was triggered using macrophages isolated from healthy human blood donors, mouse bone marrow, or tumors from either C57BL6 or athymic nude mice. While LM609 does not appear to induce phagocytosis (Figure 3F and G), several antibody therapeutics do utilize this mechanism, including anti-CD20 (rituximab) and anti-EGFR (cetuximab). Because the lung cancer cells we tested express high levels of CD47 (Figure 3F and S4B), this "don't eat me" cell surface marker [39] may account for the lack of a phagocytosis response. Indeed, the combination of cetuximab with an anti-CD47 antibody dramatically increases macrophage ADCP in preclinical models [46] and is currently being tested in clinical trials for colorectal cancer. Combining such an approach with LM609 may further enhance its activity in vivo, especially for tumors that may be particularly enriched for CD47 [47].

Interestingly, LM609 was not able to induce NK-mediated ADCC for any of the endogenous αvβ3-expressing human lung, pancreas, brain or kidney cancer cells examined. Mechanistically, we show that LM609-mediated killing utilizing macrophages requires Fcγ receptors typically found on macrophages (Figure 3C), and that macrophage depletion negates the anti-tumor effect of the antibody in vivo (Figure 2A). However, it is possible that LM609 could utilize other known ADCC effector cells including neutrophils and dendritic cells, especially since markers for these cell types show positive correlations with *ITGB3* expression in patient tissues (Figure 1A). It is more difficult to determine if the reduction of αvβ3-expressing circulating tumor cells (CTCs) in mice treated with the combination of erlotinib and LM609 (Figure 2D) is a result of macrophage-mediated ADCC within the circulation, or whether LM609 is able to reduce the aggressive nature of the primary tumor. Also, it is interesting to consider whether LM609 therapy alters the phenotype of TAMs by virtue of eliminating αvβ3-expressing tumor cells. Our work provides the rationale for a closer examination of how tumor progression and response to therapy depends on the unique relationship between TAMs and αvβ3-expressing tumor cells.

In conclusion, our study demonstrates that αvβ3-expressing tumors are enriched for macrophages and highlights how this scenario can be manipulated using antibody therapeutics to exploit these two elements (Figure 4). Indeed, an anti-αvβ3 antibody encourages macrophages to selectively destroy the αvβ3+ drug-resistant tumor cells within the primary tumor as well as CTCs, together delaying the onset of therapy resistance and potentially slowing disease progression. Because LM609 only recognizes human integrin αvβ3, utilizing human xenograft tumors in mice allows us to separate its ability to induce ADCC from any impact on host-derived macrophages or tumor-associated endothelial cells that require this integrin for angiogenesis [1, 2]. Considering that angiogenesis contributes to tumor growth, and since LM609 is an IgG1 antibody with higher affinity for human versus mouse macrophage Fcγ receptors [48], there may be additional benefits for this therapeutic strategy when applied to drug resistant tumors in humans, particularly when such agents are not combined with immunosuppressive drugs as they have been in the past [13]. In a broader sense, our work also highlights macrophage mediated ADCC as a potentially powerful approach for cancer targeted antibodies and suggests that antibody design may benefit from modifications to enable the exploitation of TAMs.

Supplementary Material

Refer to Web version on PubMed Central for supplementary material.

Acknowledgments

References

1. Brooks PC, Clark RA, Cheresh DA. Requirement of vascular integrin alpha v beta 3 for angiogenesis. Science 1994;264:569–571. [PubMed: 7512751]

2. Brooks PC, Montgomery AM, Rosenfeld M, Reisfeld RA, Hu T, Klier G, et al. Integrin alpha v beta 3 antagonists promote tumor regression by inducing apoptosis of angiogenic blood vessels. Cell 1994;79:1157–1164. [PubMed: 7528107]

3. Cooper J, Giancotti FG. Integrin Signaling in Cancer: Mechanotransduction, Stemness, Epithelial Plasticity, and Therapeutic Resistance. Cancer Cell 2019;35:347–367. [PubMed: 30889378]

4. Desgrosellier JS, Cheresh DA. Integrins in cancer: biological implications and therapeutic opportunities. Nat Rev Cancer 2010;10:9–22. [PubMed: 20029421]

5. Nabors LB, Mikkelsen T, Rosenfeld SS, Hochberg F, Akella NS, Fisher JD, et al. Phase I and correlative biology study of cilengitide in patients with recurrent malignant glioma. J Clin Oncol 2007;25:1651–1657. [PubMed: 17470857]

6. Reardon DA, Fink KL, Mikkelsen T, Cloughesy TF, O'Neill A, Plotkin S, et al. Randomized phase II study of cilengitide, an integrin-targeting arginine-glycine-aspartic acid peptide, in recurrent glioblastoma multiforme. J Clin Oncol 2008;26:5610–5617. [PubMed: 18981465]

7. Stupp R, Hegi ME, Gorlia T, Erridge SC, Perry J, Hong YK, et al. Cilengitide combined with standard treatment for patients with newly diagnosed glioblastoma with methylated MGMT promoter (CENTRIC EORTC 26071–22072 study): a multicentre, randomised, open-label, phase 3 trial. The lancet oncology 2014;15:1100–1108. [PubMed: 25163906]

8. Weller M, Nabors LB, Gorlia T, Leske H, Rushing E, Bady P, et al. Cilengitide in newly diagnosed glioblastoma: biomarker expression and outcome. Oncotarget 2016;7:15018–15032. [PubMed: 26918452]

9. Cosset E, Ilmjarv S, Dutoit V, Elliott K, von Schalscha T, Camargo MF, et al. Glut3 Addiction Is a Druggable Vulnerability for a Molecularly Defined Subpopulation of Glioblastoma. Cancer Cell 2017;32:856–868 e855. [PubMed: 29198914]

10. McNeel DG, Eickhoff J, Lee FT, King DM, Alberti D, Thomas JP, et al. Phase I trial of a monoclonal antibody specific for alphavbeta3 integrin (MEDI-522) in patients with advanced malignancies, including an assessment of effect on tumor perfusion. Clin Cancer Res 2005;11:7851–7860. [PubMed: 16278408]

11. Arbour KC, Mezquita L, Long N, Rizvi H, Auclin E, Ni A, et al. Impact of Baseline Steroids on Efficacy of Programmed Cell Death-1 and Programmed Death-Ligand 1 Blockade in Patients With Non–Small-Cell Lung Cancer. Journal of Clinical Oncology 2018;36:2872–2878. [PubMed: 30125216]

12. Comito G, Pons Segura C, Taddei ML, Lanciotti M, Serni S, Morandi A, et al. Zoledronic acid impairs stromal reactivity by inhibiting M2-macrophages polarization and prostate cancer-associated fibroblasts. Oncotarget 2017;8:118–132. [PubMed: 27223431]

13. Hersey P, Sosman J, O'Day S, Richards J, Bedikian A, Gonzalez R, et al. A randomized phase 2 study of etaracizumab, a monoclonal antibody against integrin alpha(v)beta(3), + or - dacarbazine

in patients with stage IV metastatic melanoma. Cancer 2010;116:1526–1534. [PubMed: 20108344]

14. Fujimura T, Kakizaki A, Kambayashi Y, Sato Y, Tanita K, Lyu C, et al. Cytotoxic antimelanoma drugs suppress the activation of M2 macrophages. Exp Dermatol 2018;27:64–70. [PubMed: 28833504]

15. Gasser M, Waaga-Gasser AM. Therapeutic Antibodies in Cancer Therapy. Adv Exp Med Biol 2016;917:95–120. [PubMed: 27236554]

16. Collins DM, O'Donovan N, McGowan PM, O'Sullivan F, Duffy MJ, Crown J. Trastuzumab induces antibody-dependent cell-mediated cytotoxicity (ADCC) in HER-2-non-amplified breast cancer cell lines. Ann Oncol 2012;23:1788–1795. [PubMed: 22056974]

17. Kurai J, Chikumi H, Hashimoto K, Yamaguchi K, Yamasaki A, Sako T, et al. Antibody-dependent cellular cytotoxicity mediated by cetuximab against lung cancer cell lines. Clin Cancer Res 2007;13:1552–1561. [PubMed: 17332301]

18. Carter P Improving the efficacy of antibody-based cancer therapies. Nat Rev Cancer 2001;1:118–129. [PubMed: 11905803]

19. Seguin L, Kato S, Franovic A, Camargo MF, Lesperance J, Elliott KC, et al. An integrin beta(3)-KRAS-RalB complex drives tumour stemness and resistance to EGFR inhibition. Nat Cell Biol 2014;16:457–468. [PubMed: 24747441]

20. Desgrosellier JS, Barnes LA, Shields DJ, Huang M, Lau SK, Prevost N, et al. An integrin alpha(v)beta(3)-c-Src oncogenic unit promotes anchorage-independence and tumor progression. Nat Med 2009;15:1163–1169. [PubMed: 19734908]

21. Cheresh DA, Spiro RC. Biosynthetic and functional properties of an Arg-Gly-Asp-directed receptor involved in human melanoma cell attachment to vitronectin, fibrinogen, and von Willebrand factor. J Biol Chem 1987;262:17703–17711. [PubMed: 2447074]

22. Danaher P, Warren S, Dennis L, D'Amico L, White A, Disis ML, et al. Gene expression markers of Tumor Infiltrating Leukocytes. Journal for immunotherapy of cancer 2017;5:18. [PubMed: 28239471]

23. Shu JQ G; Mohammad I A Semi-Automatic Image Analysis Tool for Biomarker Detection in Immunohistochemistry Analysis. Seventh International Conference on Image and Graphics 2013;937–942.

24. Bracher M, Gould HJ, Sutton BJ, Dombrowicz D, Karagiannis SN. Three-colour flow cytometric method to measure antibody-dependent tumour cell killing by cytotoxicity and phagocytosis. J Immunol Methods 2007;323:160–171. [PubMed: 17531261]

25. Kaneda MM, Messer KS, Ralainirina N, Li H, Leem CJ, Gorjestani S, et al. PI3Kgamma is a molecular switch that controls immune suppression. Nature 2016;539:437–442. [PubMed: 27642729]

26. Seguin L, Kato S, Franovic A, Camargo MF, Lesperance J, Elliott KC, et al. An integrin beta(3)-KRAS-RalB complex drives tumour stemness and resistance to EGFR inhibition. Nat Cell Biol 2014;16:457–468. [PubMed: 24747441]

27. Coussens LM, Werb Z. Inflammation and cancer. Nature 2002;420:860–867. [PubMed: 12490959]

28. Ruffell B, Coussens LM. Macrophages and therapeutic resistance in cancer. Cancer Cell 2015;27:462–472. [PubMed: 25858805]

29. Pathria P, Louis TL, Varner JA. Targeting Tumor-Associated Macrophages in Cancer. Trends Immunol 2019;40:310–327. [PubMed: 30890304]

30. Cheresh DA. Human endothelial cells synthesize and express an Arg-Gly-Asp-directed adhesion receptor involved in attachment to fibrinogen and von Willebrand factor. PNAS 1987;84:6471–6475. [PubMed: 2442758]

31. Gutheil JC, Campbell TN, Pierce PR, Watkins JD, Huse WD, Bodkin DJ, et al. Targeted antiangiogenic therapy for cancer using Vitaxin: a humanized monoclonal antibody to the integrin alphavbeta3. Clin Cancer Res 2000;6:3056–3061. [PubMed: 10955784]

32. Delbaldo C, Raymond E, Vera K, Hammershaimb L, Kaucic K, Lozahic S, et al. Phase I and pharmacokinetic study of etaracizumab (Abegrin), a humanized monoclonal antibody against alphavbeta3 integrin receptor, in patients with advanced solid tumors. Investigational new drugs 2008;26:35–43. [PubMed: 17876527]

33. Chung FT, Lee KY, Wang CW, Heh CC, Chan YF, Chen HW, et al. Tumor-associated macrophages correlate with response to epidermal growth factor receptor-tyrosine kinase inhibitors in advanced non-small cell lung cancer. Int J Cancer 2012;131:E227–235. [PubMed: 22174092]

34. Milano A, Mazzetta F, Valente S, Ranieri D, Leone L, Botticelli A, et al. Molecular Detection of EMT Markers in Circulating Tumor Cells from Metastatic Non-Small Cell Lung Cancer Patients: Potential Role in Clinical Practice. Anal Cell Pathol (Amst) 2018;2018:3506874. [PubMed: 29682444]

35. Jie X-X, Zhang X-Y, Xu C-J. Epithelial-to-mesenchymal transition, circulating tumor cells and cancer metastasis: Mechanisms and clinical applications. Oncotarget 2017;8:81558–81571. [PubMed: 29113414]

36. Noy R, Pollard JW. Tumor-associated macrophages: from mechanisms to therapy. Immunity 2014;41:49–61. [PubMed: 25035953]

37. Listinsky JJ, Siegal GP, Listinsky CM. Glycoengineering in cancer therapeutics: a review with fucose-depleted trastuzumab as the model. Anticancer Drugs 2013;24:219–227. [PubMed: 23059384]

38. Yu X, Marshall MJE, Cragg MS, Crispin M. Improving Antibody-Based Cancer Therapeutics Through Glycan Engineering. BioDrugs : clinical immunotherapeutics, biopharmaceuticals and gene therapy 2017;31:151–166.

39. Chao MP, Weissman IL, Majeti R. The CD47-SIRPalpha pathway in cancer immune evasion and potential therapeutic implications. Curr Opin Immunol 2012;24:225–232. [PubMed: 22310103]

40. Brown EJ, Frazier WA. Integrin-associated protein (CD47) and its ligands. Trends in Cell Biology 2001;11:130–135. [PubMed: 11306274]

41. Aras S, Zaidi MR. TAMeless traitors: macrophages in cancer progression and metastasis. Br J Cancer 2017;117:1583–1591. [PubMed: 29065107]

42. Riabov V, Gudima A, Wang N, Mickley A, Orekhov A, Kzhyshkowska J. Role of tumor associated macrophages in tumor angiogenesis and lymphangiogenesis. Front Physiol 2014;5:75. [PubMed: 24634660]

43. Trikha P, Sharma N, Pena C, Reyes A, Pecot T, Khurshid S, et al. E2f3 in tumor macrophages promotes lung metastasis. Oncogene 2016;35:3636–3646. [PubMed: 26549026]

44. Zhang B, Zhang Y, Zhao J, Wang Z, Wu T, Ou W, et al. M2-polarized macrophages contribute to the decreased sensitivity of EGFR-TKIs treatment in patients with advanced lung adenocarcinoma. Med Oncol 2014;31:127. [PubMed: 25034365]

45. Poh AR, Ernst M. Targeting Macrophages in Cancer: From Bench to Bedside. Frontiers in oncology 2018;8. [PubMed: 29450192]

46. Zhang M, Hutter G, Kahn SA, Azad TD, Gholamin S, Xu CY, et al. Anti-CD47 Treatment Stimulates Phagocytosis of Glioblastoma by M1 and M2 Polarized Macrophages and Promotes M1 Polarized Macrophages In Vivo. PLoS ONE 2016;11:e0153550. [PubMed: 27092773]

47. Noman MZ, Van Moer K, Marani V, Gemmill RM, Tranchevent LC, Azuaje F, et al. CD47 is a direct target of SNAI1 and ZEB1 and its blockade activates the phagocytosis of breast cancer cells undergoing EMT. Oncoimmunology 2018;7:e1345415. [PubMed: 29632713]

48. Guilliams M, Bruhns P, Saeys Y, Hammad H, Lambrecht BN. The function of Fcgamma receptors in dendritic cells and macrophages. Nat Rev Immunol 2014;14:94–108. [PubMed: 24445665]

Significance

Therapeutic antibodies are commonly engineered to optimize engagement of NK cells as effectors. In contrast, LM609 targets $\alpha v\beta 3$ to suppress tumor progression and enhance drug sensitivity by exploiting TAMs to trigger ADCC.

a Co-enrichment of ITGB3 (β3 mRNA) and ADCC mediators (except NK cells) for a subset of TCGA datasets

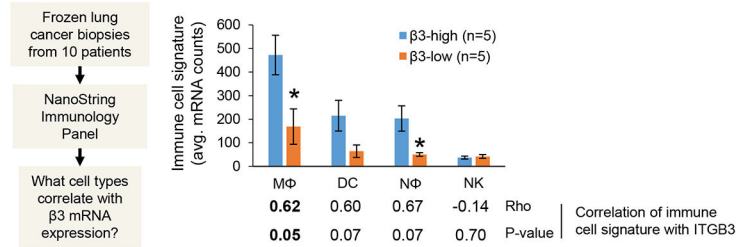*Co-enrichment of ITGB3 and macrophage markers*

	KIRP	SARC	THCA	SKCM	OV	KIRC	BRCA	GBM	LUAD	STAD	PRAD	PAAD	ESCA	CRC
MΦ	0.0	0.0	0.1	0.2	0.2	0.3	0.3	0.3	0.3	0.3	0.3	0.4	0.4	0.6
DC	0.1	0.0	0.1	0.2	0.1	0.2	0.2	0.3	0.3	0.4	0.4	0.4	0.4	0.6
NΦ	0.0	0.0	0.1	0.1	0.2	0.1	0.2	0.3	0.2	0.3	0.3	0.4	0.3	0.6
NK	0.0	0.0	0.0	0.1	0.1	-0.1	0.0	0.0	0.0	0.1	0.2	0.1	0.0	0.2

Immune cell type markers analyzed:

Macrophage (MΦ) MRC1, CD86, CD163, CD84, MS4A4A, CD68
Dendritic Cell (DC) CCL13, CD209, HSD11B1
Neutrophil (NΦ) FPR1, SIGLEC5, CSF3R, FCAR, FCGR3B, CEACAM3, S100A12
NK Cell (NK) XCL1, XCL2, NCR1

Values = Pearson correlation coefficient (gene vs. *ITGB3*)
Red fill indicates positive correlation (r ≥ 0.3)

b Co-enrichment of ITGB3 (β3 mRNA) and ADCC mediators for 10 lung cancer biopsies

Frozen lung cancer biopsies from 10 patients
↓
NanoString Immunology Panel
↓
What cell types correlate with β3 mRNA expression?

Immune cell signature (avg. mRNA counts)

β3-high (n=5)
β3-low (n=5)

	MΦ	DC	NΦ	NK	
0.62	**0.62**	0.60	0.67	-0.14	Rho — Correlation of immune cell signature with ITGB3
0.05	**0.05**	0.07	0.07	0.70	P-value

c Validation of CD68+ macrophages and β3+ tumor cells at the protein level

Lung Prostate Colorectal Kidney GBM

CD68 %positive area

CD163 % positive area

β3- β3+

samples:
Lung: n=46 (65%) n=25 (35%)
Prostate: n=34 (53%) n=30 (47%)
Colorectal: n=72 (69%) n=33 (31%)
Kidney: n=34 (71%) n=14 (29%)
GBM: n=32 (46%) n=38 (54%)

% β3+ or β3-:

β3
CD68
CD163

25 µm

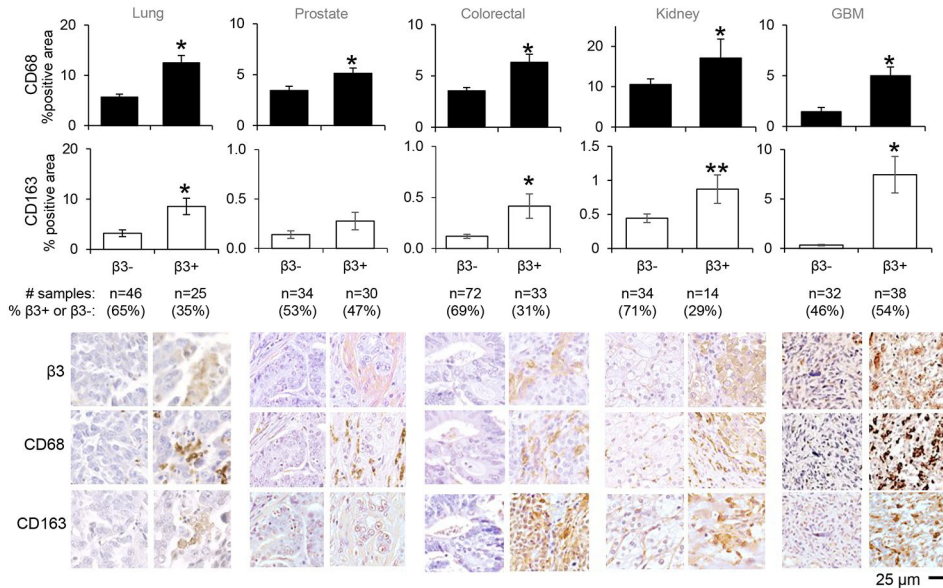**Figure 1: Integrin αvβ3-positive tumors are enriched for ADCC mediators**
(A) The correlation between *ITGB3* expression and combined markers of immune cell types was analyzed for the publicly available TCGA data sets listed in the materials and methods. The markers used for each cell type are indicated here and Supplementary Table 1. The table shows the average Pearson's correlation coefficients for tumors in each dataset using the immune cell type markers listed. MΦ; macrophage, DC; dendritic cell, NΦ; neutrophil, NK; natural killer. RNA Seq V2 RSEM datasets: KIRP = Kidney renal papillary cell carcinoma, TCGA, Provisional, 280 samples. SARC = Sarcoma, TCGA, Provisional, 241 samples. THCA = Thyroid carcinoma, TCGA, Provisional, 397 samples. SKCM = Skin cutaneous melanoma, TCGA, Provisional, 479 samples. OV = Ovarian serous cystadenocarcinoma, TCGA, Provisional, 182 samples. KIRC = Kidney renal clear cell carcinoma, TCGA,

Provisional, 534 samples. BRCA = Breast invasive carcinoma, TCGA, Provisional, 1100 samples. GBM = Glioblastoma multiforme, TCGA, Provisional, 166 samples. LUAD = Lung adenocarcinoma, TCGA, Provisional, 517 samples. STAD = Stomach adenocarcinoma, TCGA, Provisional, 415 samples. PRAD = Prostate adenocarcinoma, TCGA, Provisional, 498 samples. PAAD = Pancreatic adenocarcinoma, TCGA, Provisional, 179 samples. ESCA = Esophageal carcinoma, TCGA, Provisional, 83 samples. CRC = Colorectal adenocarcinoma, TCGA, Provisional, 382 samples.

(B) The correlation between *ITGB3* expression and combined markers of immune cell types was analyzed for biopsy samples from 10 lung adenocarcinoma patients using nCounter PanCancer Immune Panel (NanoString). Levels of immune cell type markers between β3-high and -low tissues were compared. The table below the graph shows Spearman's correlation coefficients and P-values. Mφ; macrophage, DC; dendritic cell, Nφ; neutrophil, NK; natural killer.

(C) Tumor microarray slides were stained for β3 integrin and macrophage markers, CD68 and CD163. Graphs show mean±SE for the % positive area for CD68 or CD163, grouped by β3+ vs. β3- status. The number of samples analyzed per array is indicated. *P<0.05 and **P<0.1 using Student's t test or Mann-Whitney U test compared to β3-negative. The same areas of serial sections stained for integrin β3 and macrophage markers are shown. The same areas of serial sections stained for integrin β3 and macrophage markers are shown. Bar = 25 μm.
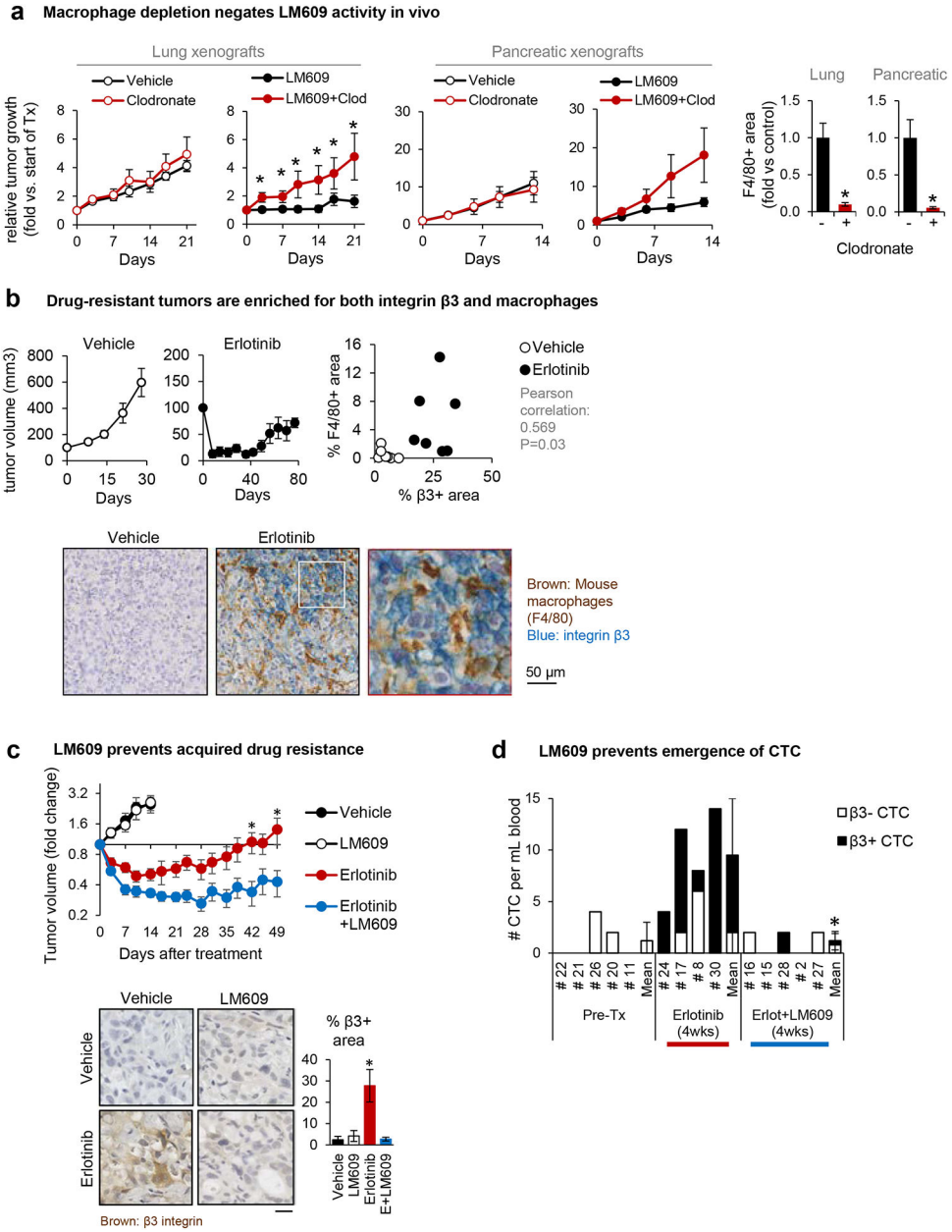
Figure 2: Anti-αvβ3 monoclonal antibody triggers macrophage-mediated tumor cell killing
(A) Nude mice were subcutaneously injected with β3-positive human tumor cells and treated
with combinations of control vs. clodronate liposome (for macrophage depletion) and PBS
vs. LM609 (the anti-αvβ3 monoclonal antibody). At the end of the study, the tumor tissues
were stained (immunofluorescence or immunohistochemistry) for a mouse macrophage
marker F4/80-positive areas to confirm macrophage depletion by the clodronate liposome.
Mean±SE is shown for 3–6 mice per group. *P<0.05 compared to control using two-tailed
Student's t test.
(B) Subcutaneous HCC827 tumors from mice treated with erlotinib or vehicle control
(Captisol) were harvested and double-stained for the mouse macrophage marker F4/80

(brown) and integrin β3 (blue). The dot plot shows the quantification of % area F4/80+ vs. β3+ area for each tumor.

(C) Mice bearing HCC827 subcutaneous flank tumors were treated with vehicle, the anti-αvβ3 LM609 (10 mg/kg), erlotinib (6.25 mg/kg), or the combination. Tumor dimensions were measured biweekly and volume calculated as $V = 1/2 \text{ (length} \times \text{width}^2)$. Graph shows mean±SE for n=5 (Vehicle, LM609) or n=9 (Erlotinib, Erlotinib+LM609) mice per group. *P<0.05 for Erlotinib vs. Erlotinib/LM609 using ANOVA. Representative pictures of tumors harvested on day 15 (Vehicle and LM609 groups, n=5) or day 50 (erlotinib and erlotinib/LM609 groups, n=5), stained for integrin β3. The β3-positive area fraction was quantified using ImageJ. Scale bar = 10 μm.. *P<0.05 for Erlotinib vs. Vehicle, LM609, and Erlotinib/LM609 using Student's t-test. Error bars indicate standard errors.

(D) Mice received orthotopic injections of luciferase- and GFP-expressing HCC827 lung cancer cells. Mice were treated with either erlotinib or erlotinib+LM609 for 4 weeks before euthanasia and circulating tumor cell (CTC) analysis. The numbers of CTC per mL blood are shown. *P<0.05 for Erlotinib+LM609 vs. Erlotinib using Student's t-test.
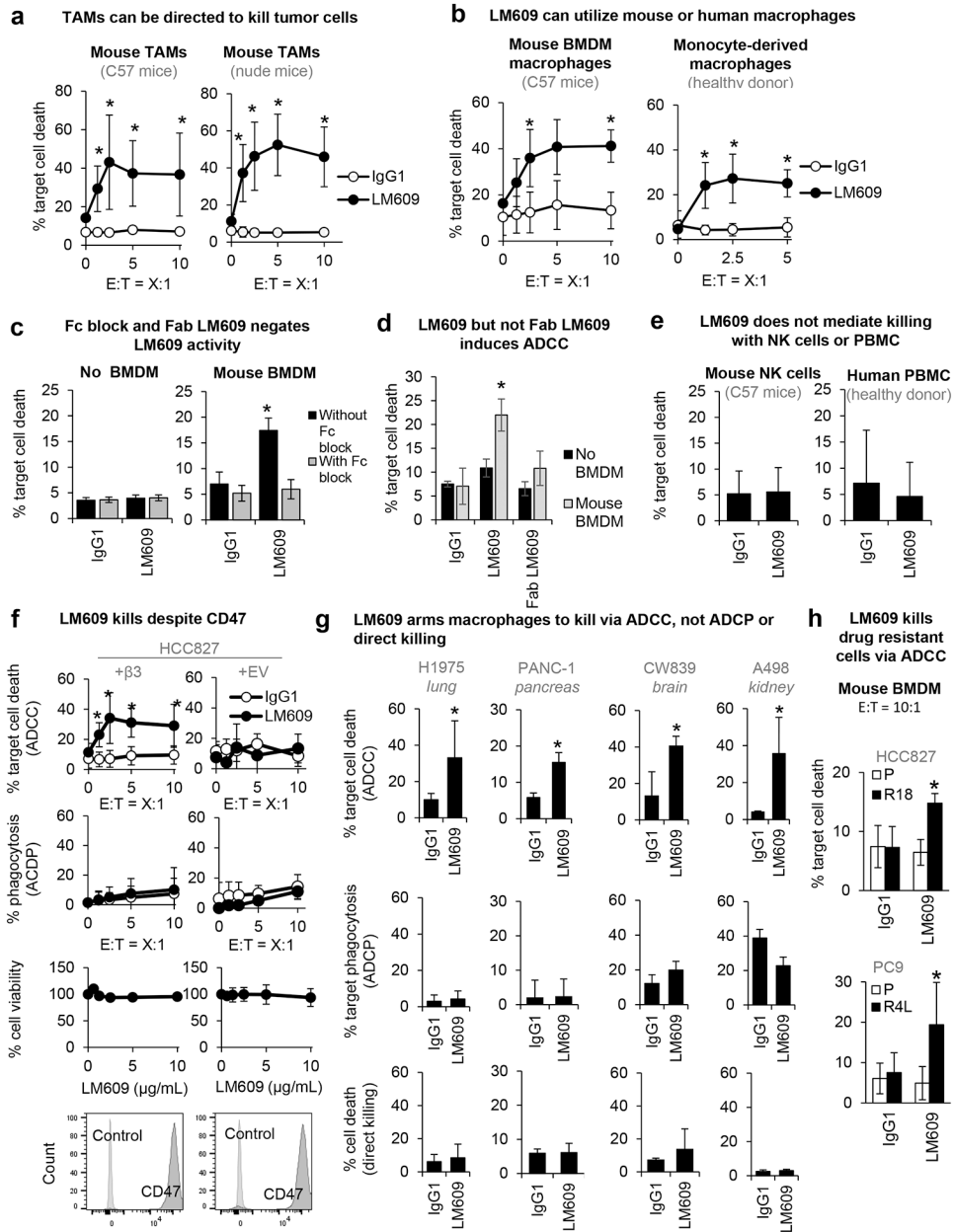
Figure 3: LM609 induces macrophage-mediated ADCC, not phagocytosis

(A) Mouse tumor-associated macrophages (TAMs) are tested for ADCC activity. Graphs show mean±SD of % target cell (HCC827+β3) death at indicated effector-to-target cell ratios (E:T) induced by anti-αvβ3 LM609 (10 μg/mL) vs. IgG control. *P<0.05 compared to IgG1 using Student's t test (repeated at least 3 times). Error bars indicate standard deviation. (B) Human monocyte-derived macrophages (donor 631) and mouse bone marrow-derived macrophages (BMDM) are tested for their effects on target cells (HCC827+β3) for a range of E:T ratios. Tumor cell killing induced by anti-αvβ3 LM609 (10 μg/mL) vs. IgG control was measured. Error bars indicate standard deviation. *P<0.05 compared to the IgG1 group using Student's t test (repeated at least 3 times).

(C) Death of target cells (HCC827+β3) induced by LM609 (10 μg/mL) in the absence or presence of BMDM (E:T=10:1) was evaluated in the absence or presence of function blocking antibodies targeting Fcγ receptors (Fc block). Error bars indicate standard deviation. *P<0.05 compared to IgG using Student's t test (n=4).

(D) Death of target cells (HCC827+β3) induced by LM609 or Fab LM609 (10 μg/mL) in the absence or presence of BMDM (E:T=10:1) was evaluated. Error bars indicate standard deviation. *P<0.05 compared to IgG using Student's t test (n=4).

(E) Death of target cells (HCC827+β3) measured after the co-incubation with mouse NK cells (E:T=5:1) and human PBMCs (E:T=500:1) with and without LM609 (10 μg/mL). Error bars indicate standard deviation.

(F) ADCC, ADCP, MTT assays, and flow cytometry for CD47 expression were performed for HCC827 cells with ectopic expression of empty vector (+EV) or the integrin β3 subunit (+β3). Death of target cells induced by LM609 (10 μg/mL) in the presence of mouse BMDM was evaluated at a range of E:T ratios (ADCC). Phagocytosis of target cells induced by LM609 (10 μg/mL) in the presence of mouse BMDM was evaluated (ADCP). Death of target cells induced by LM609 without effector cells was evaluated (% cell viability). CD47 expression on the target cells are shown. Error bars indicate standard deviation. *P<0.05 compared to IgG using Student's t test (n= at least 3).

(G) ADCC, ADCP, and viability assays were performed for a panel of cancer cell lines with endogenous αvβ3 expression. Death of target cells induced by LM609 (10 μg/mL) in the presence of mouse BMDM was evaluated at an E:T ratio of 5:1 (ADCC). Phagocytosis of target cells induced by LM609 (10 μg/mL) in the presence of mouse BMDM was evaluated (ADCP). Direct killing of target cells by LM609 (10 μg/mL) was evaluated by measuring PI-positive cells after the 5 hr incubation of the target cells and LM609. Error bars indicate standard deviation. *P<0.05 compared to IgG using Student's t test (n= at least 3).

(H) ADCC assay was performed for drug resistant cells with endogenous αvβ3 expression and drug sensitive cells with no αvβ3. Death of target cells induced by LM609 (10 μg/mL) in the presence of mouse BMDM was evaluated at an E:T ratio of 5:1. *P<0.05 compared to IgG using Student's t test (n= at least 3).
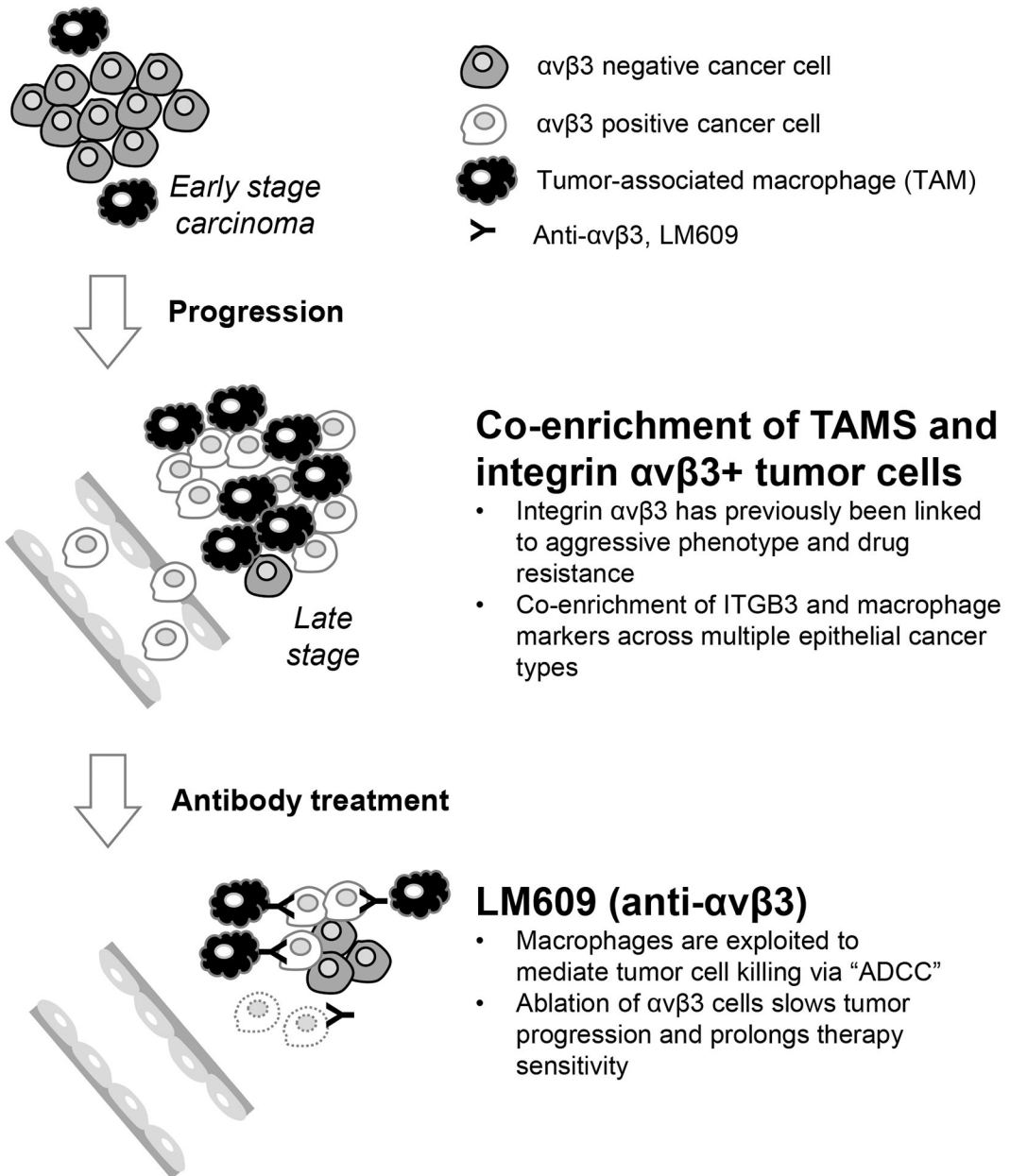
Figure 4: Working model

The anti-αvβ3 antibody (LM609) engages tumor-associated macrophages to eliminate aggressive αvβ3+ cancer cells by triggering antibody-dependent cellular cytotoxicity (ADCC).